BIOCHEMISTRY
including biophysical chemistry & molecular biology
Article

Biochemistry **2010,** *49,* 9171–9180 9171
DOI: 10.1021/bi101184g

Sensing DNA Opening in Transcription Using Quenchable Förster Resonance Energy Transfer†

Thorben Cordes,‡ Yusdi Santoso,‡ Alexandra I. Tomescu,‡ Kristofer Gryte,‡ Ling Chin Hwang,‡,∥ Beatriz Camará,§ Sivaramesh Wigneshweraraj,§ and Achillefs N. Kapanidis*,‡

‡*Biological Physics Research Group, Department of Physics, University of Oxford, Clarendon Laboratory, Parks Road, Oxford OX1 3PU, United Kingdom, and* §*Division of Microbiology, Department of Medicine, Faculty of Medicine and Centre for Molecular Microbiology and Infection, Flowers Building, Imperial College London, London SW7 2AZ, United Kingdom.* ∥*Present address: Laboratory of Molecular Biology, National Institute of Diabetes and Digestive and Kidney Diseases, National Institutes of Health, Bethesda, MD 20892.*

Received July 27, 2010; Revised Manuscript Received September 3, 2010

ABSTRACT: Many biological processes, such as gene transcription and replication, involve opening and closing of short regions of double-stranded DNA (dsDNA). Few techniques, however, can study these processes in real time or at the single-molecule level. Here, we present a Förster resonance energy transfer (FRET) assay that monitors the state of DNA (double- vs single-stranded) at a specific region within a DNA fragment, at both the ensemble level and the single-molecule level. The assay utilizes two closely spaced fluorophores: a FRET donor fluorophore (Cy3B) on the first DNA strand and a FRET acceptor fluorophore (ATTO647N) on the complementary strand. Because our assay is based on quenching and dequenching FRET processes, i.e., the presence or absence of contact-induced fluorescence quenching, we have named it a "quenchable FRET" assay or "quFRET". Using *lac* promoter DNA fragments, quFRET allowed us to sense transcription bubble expansion and compaction during abortive initiation by bacterial RNA polymerase. We also used quFRET to confirm the mode of action of gp2 (a phage-encoded protein that acts as a potent inhibitor of *Escherichia coli* transcription) and rifampicin (an antibiotic that blocks transcription initiation). Our results demonstrate that quFRET should find numerous applications in many processes involving DNA opening and closing, as well as in the development of new antibacterial therapies involving transcription.

Processes that open and close duplex DNA regions are essential in many fundamental biological processes such as gene transcription and replication (*1*). For example, promoter opening is an obligatory step for transcription and serves as the first step in gene expression. During transcription initiation in *Escherichia coli*, RNA polymerase (RNAP) binds to a double-stranded promoter DNA region to form a closed complex (RP_c). At most promoters, this reaction is followed by isomerization in which double-stranded DNA (dsDNA) is partially opened ("melted") to form a "transcription bubble" that comprises two single-stranded DNA (ssDNA) regions; this RNAP−promoter DNA complex is known as the "open complex" (RP_o) and is transcriptionally active (*2*, *3*). Upon formation of RP_o, RNAP can access the information encoded in the specific template sequence and perform template-directed gene transcription (*3*, *4*).

Opening and closing of promoter DNA have been studied using a variety of biochemical and biophysical assays (*5*). Standard methods use chemical probes that exploit the different reactivity of specific nucleotides (e.g., thymines and cytosines) in the dsDNA and ssDNA forms; these assays include permanganate footprinting (*6*), cytosine methylation (*7*), and hydroxyl radical footprinting (*8*, *9*). Other assays look at the pre-steady-state kinetics of the formation of the first phosphodiester bond, which occurs at the start of transcription; typically, this assay monitors the formation of a bond between an initiating dinucleotide and the nucleotide complementary to the third base on the template strand. These assays were initially performed using radioactive nucleotides (*10*) and subsequently converted into fluorescence-based assays (*11*, *12*). These assays, however, are indirect and based on the assumption that the rate-limiting step is RP_o formation and not the initiation of RNA synthesis; moreover, these assays cannot report on intermediates populated during promoter opening.

Assays using ensemble fluorescence spectroscopy relied on quantum yield changes of either aminopurine (*13*−*15*) or coumarin (*12*) derivatives incorporated into the DNA region that melts upon RP_o formation. Though useful for determining important parameters such as binding constants, these methods use fluorophores characterized by low signal intensities and thus cannot be used for single-molecule studies, which are highly desirable for capturing detailed views of the real-time kinetics, molecular dynamics, and heterogeneity in biological mechanisms (*16*). Other attempts such as protein-induced fluorescence enhancement (PIFE) monitor changes in the fluorescence intensity of a single fluorophore; such changes correlate with the proximity of the unlabeled protein (*17*).

†T.C. was supported by a Marie-Curie Intra-European Fellowship provided by the European Commission under the Seventh Framework Programme (Grant PIEF-GA-2009-255075). Y.S. was supported by an EPA Cephalosporin Scholarship (Linacre College, University of Oxford), A.I.T. by a Medical Research Council Doctoral Training Award (Department of Physics, University of Oxford), and K.G. by a Clarendon Graduate Fellowship (University of Oxford). S.W. is a recipient of a BBSRC David Phillips Fellowship (BB/E023703). A.N.K. was supported by European Commission Seventh Framework Programme (FP7/2007-2013) Grant HEALTH-F4-2008-201418 (entitled READNA) and BBSRC Grant BB/H01795X/1.

*To whom correspondence should be addressed. E-mail: a.kapanidis1@physics.ox.ac.uk. Fax: +44-1865-272-401. Phone: +44-1865-272-400.

Published on Web 09/06/2010

Recently, a single-molecule assay based on magnetic tweezers (*5*) was introduced to study RP_o formation as well as transcription initiation, promoter escape, and elongation (*18*). This impressive assay showed that conformational changes in DNA ("DNA scrunching", i.e., formation and dissolution of transient DNA loops and bulges within the transcription bubble) are needed for RNAP to break its strong interactions with the promoter and escape into elongation. The temporal resolution of this technique, however, was limited to ≈1 s, complicating the observation of individual steps during initial transcription or of individual events of RNA synthesis. Moreover, monitoring multiple coordinates within transcription complexes using combinations of magnetic tweezers with other methods presents difficult experimental challenges (*19*). Consequently, observing the coupling of conformational changes in DNA with RNAP structural rearrangements has not been possible. Access to such information would illuminate the mechanisms of promoter opening and initial transcription in many interesting transcription systems, such as σ^{54}-dependent transcription (*20*) or eukaryotic transcription initiation (*21*).

Here, we introduce a versatile promoter opening assay based on Förster resonance energy transfer (FRET); the assay monitors DNA opening within a specific region of any DNA fragment, at the ensemble and single-molecule levels, by employing a FRET donor fluorophore on one DNA strand and a FRET acceptor fluorophore in the proximity of the donor (< 2 nm) on the complementary strand. To study RP_o formation and initial transcription, the fluorophores are placed within the region of transcription bubble formation. Fluorophore proximity causes contact-induced quenching, suppressing fluorescence and hence FRET in the dsDNA form. Upon RP_o formation (i.e., when the DNA strands within the transcription bubble are separated), contact-induced quenching is removed and a strong increase in fluorophore brightness and a high FRET efficiency is observed. Because our assay is based on quenching and dequenching FRET processes, i.e., the presence or absence of contact-induced quenching, respectively, we have named it a "quenchable FRET" (quFRET). Using *lac* promoter DNA fragments, we demonstrate that quFRET can probe the compaction and expansion of the transcription bubble. Finally, we use quFRET to study the mode of action of specific inhibitors of bacterial RNAP in transcription initiation. Our results clearly demonstrate that quFRET can serve as a useful tool for studying DNA opening and closing, as well as biomolecules that modulate these two processes.

MATERIALS AND METHODS

DNA and Reagents. Unless otherwise stated, reagents of luminescent grade were used as received. Amino-modified oligonucleotides (IBA) were internally labeled with NHS-conjugated fluorophores Cy3B and ATTO647N (Invitrogen and ATTO-TEC) according to published protocols and purified using a liquid chromatography system (AKTA, GE Healthcare). Labeled and purified DNA single strands were annealed in hybridization buffer [50 mM Tris-HCl (pH 8.0), 1 mM EDTA, and 500 mM NaCl]. The two different DNA fragments will be called $lac^{Cy3B,X/ATTO647N,Y}$ (donor fluorophore at position *X* and acceptor fluorophore at position *Y* with respect to transcription start site named +1) throughout this work. The DNA sequence (Figure 1a) is derived from a *lac* consensus promoter DNA to which bacterial RNA polymerase binds. For a photophysical characterization and comparison experiments, we used a DNA sample with an 18 bp separation between Cy3B and ATTO647N (*22*). The sequences of these oligonucleotides (IBA) are shown in Figure S1 of the Supporting Information.

Formation of the RNA Polymerase Open Complex and Initial Transcribing Complexes. The open complex (RP_o) of *E. coli* RNA polymerase was formed according to published procedures (*16*, *23*, *24*). Briefly, dsDNA (10 nM), rifampicin [0 or 250 nM (Sigma Aldrich)], and RNAP holoenzyme [50 nM (Epicentre or USB)] were mixed in a total volume of 20 μL of KG7 buffer [40 mM HEPES-NaOH (pH 7), 100 mM potassium glutamate, 10 mM $MgCl_2$, 1 mM DTT, 100 μg/mL BSA, 5% glycerol, and 1 mM mercaptoethylamine] and incubated at 37 °C for 15 min. Subsequently, heparin Sepharose [1 mg/mL (GE Healthcare)] was added to disrupt nonspecific RNAP−DNA complexes and remove free RNAP. After 30 s at 37 °C, the samples were centrifuged, and 13 μL of supernatant was transferred to a prewarmed tube; then 9.5 μL of supernatant was subsequently transferred to a different tube, supplemented with either 500 μM ApA (for $RP_{itc,2}$), 500 μM ApA and 50 μM UTP (for $RP_{itc,4}$), 500 μM ApA, 50 μM UTP, and 50 μM GTP (for $RP_{itc,7}$), or 500 μM ApA, 50 μM UTP, 50 μM GTP, and 50 μM ATP (a mix capable of forming $RD_{e,11}$) for a total reaction volume of 10 μL. Before each single-molecule experiment, transcription complex samples were incubated for a further 20 min at 37 °C.

RNAP Functional Assay Using in Vitro Transcription and Radioactive Nucleotides. RP_o was formed in T8 buffer [50 mM Tris-HCl (pH 8.0), 100 mM KCl, 10 mM $MgCl_2$, 100 μg/mL BSA, 1 mM DTT, and 5% glycerol] as described in the previous section. Heparin Sepharose (1 mg/mL) was added to the reaction mixtures; they were incubated for 30 s at 37 °C and centrifuged for 10 s, after which 5 μL of the supernatant was transferred to a prewarmed tube. The in vitro transcription reaction mixtures were set up by adding 1 μL of supernatant to 4 μL of KG7 buffer [40 mM HEPES-NaOH (pH 7), 100 mM potassium glutamate, 10 mM $MgCl_2$, 100 μg/mL BSA, 1 mM DTT, 1 mM MEA, and 5% glycerol] supplemented with 4 units of SUPERase-In [20 units/μL (Ambion, Inc.)], 500 μM ApA, 50 μM UTP ($RP_{itc,7}$) or 50 μM UTP, 50 μM CTP, and 50 μM ATP (full transcript) in the presence of 0.3 μCi/μL [α-^{32}P]GTP [10 μCi/μL (Perkin Elmer)] and incubated for 5 min at 37°C. Reactions were stopped by addition of 1 reaction volume of loading dye [80% (v/v) formamide, 10 mM EDTA, 0.04% (w/v) bromophenol blue, and 0.04% (w/v) xylene cyanol FF], and mixtures were incubated for 5 min at 95 °C, electrophoresed on a 6 M urea−25% polyacrylamide sequencing gel, and visualized by autoradiography. To ensure an RNase-free environment, the labware used was cleaned with RNaseZap wipes or solution (Ambion, Inc.); RNase-free solutions were prepared in the laboratory, filtered, and autoclaved, using only sterile (RNase-free) tubes and glassware.

gp2−RNA Polymerase Interaction Assay Using Gel Electrophoresis. Inhibition of transcription complexes by gp2 was studied by incubation of 50 nM RNAP with 1 μM gp2 for 20 min at 37 °C, after which 10 nM promoter DNA was added, followed by incubation for 15 min at 37 °C (route 1). Alternatively, 1 μM gp2 was incubated for 15 min at 37 °C with preformed RP_o (route 2). A fraction of each reaction mixture was challenged with 1 mg/mL heparin Sepharose. The resulting samples were used in single-molecule experiments or gel electrophoresis. For gel electrophoresis, 5 μL of each sample (reaction mixture or supernatant with 0.5 μL of 50% glycerol added) was run on a 4.5% native polyacrylamide gel.

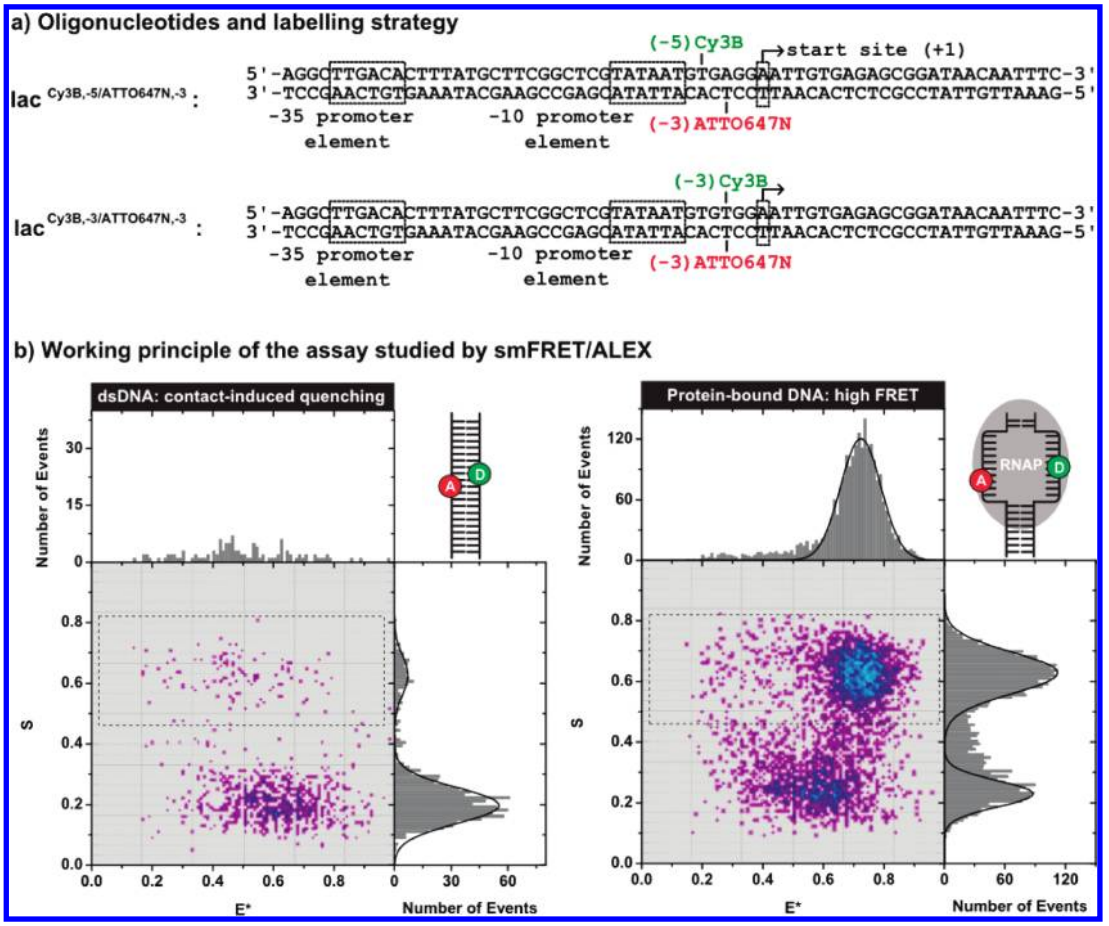

FIGURE 1: Oligonucleotide sequences and working principle of quFRET. (a) Oligonucleotide sequences of the lacCONS+2 DNA fragments used in our study. (b) Detection of RP_o formation using quFRET on fragment $lac^{Cy3B,-5/ATTO647N,-3}$ by smFRET/ALEX spectroscopy. Two fluorophores are attached in close proximity on each strand of a dsDNA (left panel). Because of their fluorescence properties, they can act as a FRET pair, but the proximity suppresses the fluorescence of both probes in dsDNA. Upon RP_o formation, high FRET values are observed (right panel). Transcription complexes were formed as described in Materials and Methods. Two-dimensional E^*/S histograms were derived from data of diffusing molecules at 37 °C at a DNA concentration of ≈50−100 pM. The measurement time was ≈20 min for panels a and b.

Ensemble Absorption and Fluorescence Spectroscopy. Absorption spectra were recorded on a standard absorption spectrometer (Cary 50 Bio, Varian).

Fluorescence spectra were recorded using a scanning spectrofluorometer (PTI). The average configuration for recording spectra was a 1 s integration time per 1 nm wavelength interval over a total range of several hundred nanometers. Excitation was performed at 533 nm (Cy3B) or 640 nm (ATTO647N). Studies were performed on $lac^{Cy3B,-5/ATTO647N,-3}$ (Figure 1a) or singly labeled versions of the promoter bearing either Cy3B or ATTO647N. Fluorescence time traces collected to monitor transcription complex formation were recorded at 37 °C in either 1 or 5 s intervals using excitation at 533 nm and detection at 660 nm. A cuvette with a path length of 1 cm and a total volume of ≈50 μL was used in combination with a heating bath that controlled the temperature within ±1 °C.

Fluorescence anisotropies r were calculated at the emission maxima of the fluorophores (for Cy3B, λ_{ex} = 540 nm and λ_{det} = 580 nm; for ATTO647N, λ_{ex} = 640 nm and λ_{det} = 670 nm) from the emission components I_{VV} and I_{VH} [where the subscripts denote the orientation, vertical (V) or horizontal (H), of the excitation and emission polarizers] according to the relationship $r = (I_{VV} - GI_{VH})/(I_{VV} + 2GI_{VH})$ (*25*). The sensitivity of the spectrometer for different polarizations was corrected using horizontal excitation where $G = I_{HV}/I_{HH}$.

Single-Molecule Fluorescence Spectroscopy. For single-molecule fluorescence and FRET, a custom-built confocal microscope was used as described previously (*26*, *27*). The setup allowed alternating-laser excitation of donor and acceptor fluorophores (*28*, *29*). The fiber-coupled output of a green [532 nm (Samba, Cobolt)] and red laser [638 nm (Cube Coherent)] was alternated with a modulation frequency of 10 kHz. The spatially filtered beams were coupled into an inverted confocal microscope [IX71 (Olympus)] equipped with an oil-immersion objective [60×, 1.35 NA, UPLSAPO 60XO (Olympus)]. The average excitation intensities for measurements were 250 μW at 532 nm and 50 μW at 640 nm. The resulting fluorescence was collected using the same objective, separated from excitation light by a dichroic mirror, focused onto a 200 μm pinhole, and split spectrally on two avalanche photodiodes [SPCM-AQR-14 (PerkinElmer)] detecting the donor and acceptor fluorescence with appropriate spectral filtering (green for 585DF70 and red for 650LP). The detector signal was registered and evaluated using custom LabVIEW software. The temperature of the sample was controlled within ±1 °C via a heating bath in combination with a custom-made heated collar attached to the objective. Unless stated otherwise, all single-molecule measurements were taken at 37 °C.

Data Analysis. Fluorescence photons arriving at the two detection channels (donor detection channel, D_{em}; acceptor detection channel, A_{em}) were assigned to either donor (D_{exc}) or acceptor (A_{exc}) excitation on the basis of their photon arrival time as described previously (*28*, *29*). Fluorophore stoichiometries S and apparent FRET efficiencies E^* were calculated for each

fluorescent burst above a certain threshold, yielding a two-dimensional (2D) histogram. Here, S is defined as the ratio of the overall green fluorescence intensity to the total green and red fluorescence intensity and describes the ratio of donor-to-acceptor fluorophores in the sample (*28*, *29*). Uncorrected FRET efficiency E^* [defined as $D_{exc}A_{em}/(D_{exc}A_{em} + D_{exc}D_{em})$] monitors the proximity between the two fluorophores. Using published procedures to identify bursts corresponding to single molecules (*30*), we obtained bursts characterized by three parameters (M, T, and L). A fluorescent signal is considered a burst provided it meets the following criteria: a total of L photons having M neighboring photons within a time interval of T microseconds. Unless stated otherwise, we identified acceptor-containing molecules by applying a burst search on $A_{exc}A_{em}$ using an M of 7, a T of 500 μs, and an L of 12; additional per-bin thresholds removed spurious changes in fluorescence intensity and selected for bright donor−acceptor molecules ($A_{exc}A_{em} > 30-50$ photons). Binning the detected bursts into a 2D E^*-S histogram allowed us to separate molecules labeled with only an acceptor fluorophore ($S \approx 0.2$) from molecules with both fluorophores present ($S \approx 0.6$; see the dashed rectangle in Figure 1a). The one-dimensional (1D) E^* distribution for donor−acceptor species was obtained by using a $0.45 < S < 0.8$ threshold; the E^* distributions were then fitted using a Gaussian function, yielding the mean E^* value for the distribution and an associated standard deviation σ.

RESULTS AND DISCUSSION

Sensing RP_o Formation Using quFRET. Our assay relies on the proximity (<2 nm) of two fluorophores; because this proximity is disrupted upon strand separation and transcription bubble formation, we reasoned that the assay can be used to study RP_o formation and related processes. Our fluorophore pair comprises a "green" and a "red" fluorophore (i.e., excited by green and red excitation wavelengths, respectively) that can participate in FRET; the FRET pair in our experiments consists of Cy3B (donor) and ATTO647N (acceptor). When the fluorophores are on fully double-stranded DNA, their fluorescence is quenched because of transient or static contacts between the fluorophores, whereas upon DNA separation in the region of the fluorophores (i.e., DNA becomes partially single-stranded), contact-induced quenching is replaced by the occurrence of FRET; the FRET efficiency can then report on the extent of local DNA opening.

To demonstrate the principle of the quFRET assay, we monitored RP_o formation on *lac* promoter DNA fragments. We prepared a DNA fragment carrying the donor on the nontemplate strand at position −5 and the acceptor on the template strand at position −3, both positions being relative to the transcription start site; this DNA was named $lac^{Cy3B,-5/ATTO647N,-3}$. The chosen labeling sites place the fluorophores in close proximity [<2 nm (Figure 1a)] and within the DNA segment that gives rise to the transcription bubble (Figure 1a,b).

The considerable size of the organic fluorophores used for quFRET has the potential to perturb the system under study; to establish whether fluorophore labeling interfered with important RNAP functions (RP_o formation, initial transcription, and promoter escape), we performed in vitro transcription assays in the presence of radioactive nucleotides. The results showed that RNAP synthesizes similar amounts of abortive products regardless of the presence or absence of labels on the template DNA; however, the labeled construct led to an increased level of promoter escape (Figure S2 of the Supporting Information). This tendency is probably attributable to slight destabilization of the transcription complexes when fluorophores are present. Such perturbation may be a concern, but in determining kinetic rate constants for promoter opening between our *lac* fragment and *lac*UV5 DNA studied in earlier work (see ref *12* and Monitoring the Kinetics of Promoter Opening Using quFRET), we found that promoter opening is not significantly affected. Because (i) a similar ladder of abortive products was obtained from unlabeled fragments, (ii) rates of promoter opening were in agreement with previous studies, and (iii) we see only apparent enhanced promoter escape, we reasoned that introduction of fluorophores within the transcription bubble did not significantly interfere with the biological activity of our studied system. Initial transcribing complexes were fully active, and any insights and conclusions obtained from our experiments are not affected by an increased level of promoter escape.

To detect RP_o formation, we performed single-molecule FRET spectroscopy with alternating-laser excitation [ALEX (*28*, *29*)] on diffusing molecules of dsDNA and RP_o (Figure 1b). After identifying single fluorescent molecules, we used their fluorescence intensities to construct a 2D histogram of apparent FRET efficiency (E^*) and relative probe stoichiometry (S) (*28*, *29*). For free double-stranded DNA molecules that carry a fluorescent acceptor, we observe two main species: a major subpopulation (≈85% of all molecules) with a low S value of <0.4, corresponding to acceptor-only species, and a minor subpopulation with intermediate S value ($0.45 < S < 0.8$; ≈15% of all molecules), corresponding to donor−acceptor species. The 1D E^* histogram for the donor−acceptor species (corresponding to the dotted rectangle in Figure 1b) shows a broad and unstructured FRET distribution characterized by the absence of high-FRET species ($E^* > 0.9$), which were expected to appear if contact-induced quenching was absent (e.g., see Figure 3). The number of detected molecules is only ≈120 (Figure 1b, left panel), a low number upon comparison of $lac^{Cy3B,-5/ATTO647N,-3}$ to a dsDNA standard carrying the same fluorophores with an 18 bp separation; this probe showed ≈1500 detected molecules with intermediate S values (Figure S3a of the Supporting Information).

Upon RP_o formation, we observed three major changes in the E^*-S histogram. First, the relevant fraction with intermediate S values increases substantially (from ≈15 to ≈60% of all molecules). Second, a population with a high E^* is observed [$E^* \approx 0.7$ (Figure 1b, right panel)]. Third, the number of detected molecules with intermediate S values increases substantially. These changes are consistent with removal of the contact-induced quenching between the fluorophores upon RP_o formation, presumably due to the separation of the two DNA strands. These observations and the quenching hypothesis are further supported by comparing the photon counting histograms [PCH (Figure S4 of the Supporting Information)] of dsDNA and RP_o from Figure 1, which were recorded for comparable concentrations (50−100 pM) and measurement times of 20 min. Upon RP_o formation, the PCHs show a significant increase in the total number of events for all three channels (Figure S4a−c of the Supporting Information, $D_{ex}D_{em}$, $A_{ex}A_{em}$, $D_{ex}A_{em}$). The mean number of detected photons in a burst also increases significantly for FRET [$D_{ex}A_{em}$, mean of ≈60 photons (Figure S4c of the Supporting Information)] and acceptor-direct-excitation photons [$A_{ex}A_{em}$, mean of ≈30 photons (Figure S4b of the Supporting Information)] pointing to removal of contact-induced quenching upon RP_o formation.

Analyzing the data to retain all fluorescent bursts (donor-only, acceptor-only, and donor−acceptor species) reveals that in the

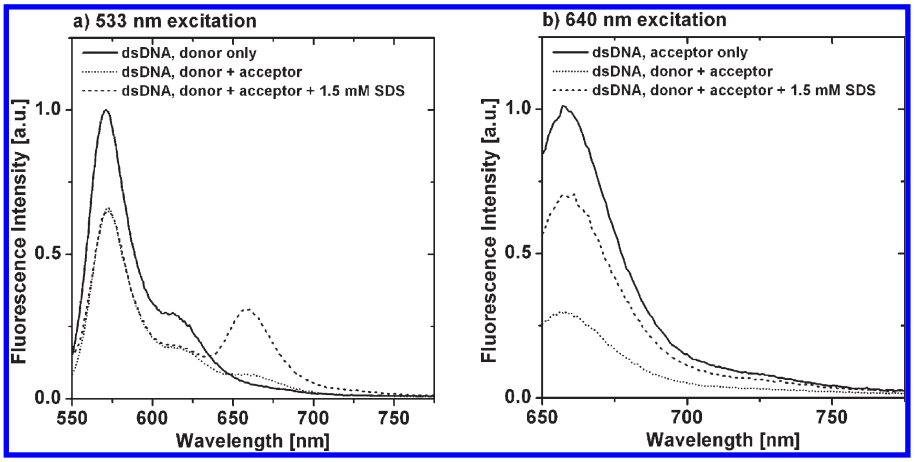

FIGURE 2: Fluorescence emission spectra of lac$^{Cy3B,-5/ATTO647N,-3}$. All spectra were recorded at 20 nM dsDNA at either 533 nm (a) or 640 nm (b) excitation. The emitted fluorescence under different buffer conditions is indicated in the figure (PBS buffer with 1 mg/mL BSA and PBS/BSA mixture with added SDS as indicated in the figure). The integration time was 1 s at 1 nm wavelength intervals.

quenched form of lac$^{Cy3B,-5/ATTO647N,-3}$, a substantial apparent fraction of the molecules (80%) is due to donor-only species, followed by acceptor-only (15%) and donor−acceptor (5%) species (Figure S5 of the Supporting Information, left panel; note that the fractions are not corrected for the different brightnesses of the two fluorophores). Upon formation of the open complex, we observe a significant increase in both the number of FRET events and their signal intensity, with ≈50% of all molecules being donor−acceptor species, ≈40% donor-only species, and ≈10% acceptor-only species. These results suggest that the quenching process mainly affects the acceptor fluorophore. We additionally observe a "smear" from the FRET to the donor-only population; this smear is likely caused by blinking and photobleaching of the acceptor fluorophore (*25*, *31*).

To show that quFRET does not depend on the exact positions of the fluorophores (provided that they are within the range for contact-mediated quenching, < 2 nm), we examined a variant of our DNA carrying the two fluorophores at different positions within the transcription bubble (lac$^{Cy3B,-3/ATTO647N,-3}$, with Cy3B and ATTO647N at position −3 on the nontemplate and template strands, respectively). The results obtained for this dsDNA and its corresponding RP_o were essentially identical to the results obtained for lac$^{Cy3B,-5/ATTO647N,-3}$: quenching for dsDNA and high E^* for RP_o (Figure S6a,b of the Supporting Information).

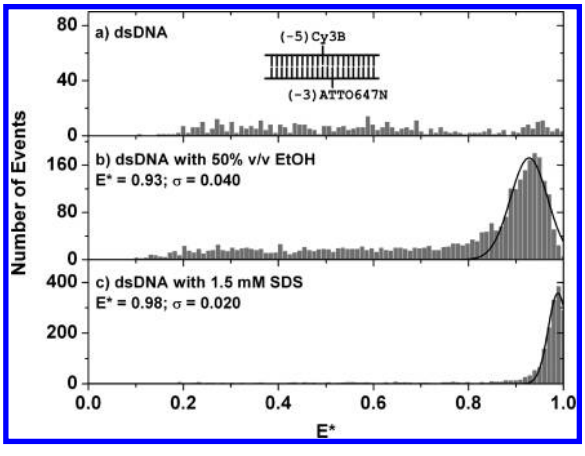

FIGURE 3: Fluorophore dequenching by ethanol and SDS. ALEX-based E^* histograms obtained from single diffusing molecules of lac$^{Cy3B,-5/ATTO647N,-3}$ at 22 °C at a concentration of ≈50−100 pM for different buffer conditions: (a) in PBS buffer with 1 mg/mL BSA, (b) in a mixture of PBS buffer, 1 mg/mL BSA, and 50% (v/v) ethanol, and (c) in PBS with 1.5 mM SDS. Measurement times were 30 min for panels a and c and 60 min for panel b.

Characterization of Fluorophore−Fluorophore Interactions in quFRET. To characterize the process responsible for our single-molecule fluorescence observables, we used ensemble fluorescence spectroscopy to examine fluorophore emission spectra under nonquenching and quenching conditions (Figure 2).

The emission spectrum of Cy3B on dsDNA in the absence of ATTO647N (Figure 2a, lac$^{Cy3B,-5}$) shows a maximum at 570 nm and a shoulder at ≈615 nm. On the other hand, lac$^{Cy3B,-5/ATTO647N,-3}$ with both fluorophores on DNA shows a similar spectral profile with an additional shoulder at ≈660 nm, but with ≈35% decreased emission intensity (Figure 2a, dotted line). Adding 1.5 mM anionic surfactant [sodium dodecyl sulfate (SDS)] leaves the intensity of Cy3B unaffected but strongly increases the long-wavelength emission centered at ≈660 nm (Figure 2a, dashed line). This long-wavelength emission is due to FRET processes in ATTO647N (Figure 2b).

On the other hand, the emission spectrum of ATTO647N in the absence of Cy3B (Figure 2b) shows a maximum at ≈660 nm and a broad emission tail extending beyond 700 nm. As for Cy3B, the ATTO647N emission is reduced by 70% for lac$^{Cy3B,-5/ATTO647N,-3}$ (Figure 2b, dotted line); moreover, dequenching by 60% is observed upon addition of 1.5 mM SDS (Figure 2b, dashed line). Interestingly, the signal intensity of Cy3B in lac$^{Cy3B,-5/ATTO647N,-3}$ is constant upon addition of SDS (Figure 2a, dotted line vs dashed line), likely because of the combined effects of dequenching of Cy3B (that increases Cy3B fluorescence intensity) and an increase in the level of FRET (that decreases Cy3B fluorescence intensity).

Interactions of the fluorophores and the protein−DNA complex were additionally investigated using anisotropy measurements. As expected, we find low anisotropies for the free dyes Cy3B (r = 0.05 ± 0.02) and ATTO647N (r = 0.08 ± 0.02) in aqueous solution. An increase to r values of 0.22 ± 0.02 (Cy3B) and 0.18 ± 0.02 (ATTO647N) was found for lac$^{Cy3B,-5/ATTO647N,-3}$; these values for dsDNA were identical for Cy3B-only and ATTO647N-only forms on the *lac* promoter. A large anisotropy increase is observed for both dyes upon RP_o formation (for Cy3B, r = 0.31 ± 0.03; for ATTO647N, r = 0.30 ± 0.04). Our results indicate the strong influence of the protein environment on the rotational freedom of the fluorophores. Thus, assigning FRET changes during and after

RP_o formation purely to changes in intraprobe distances is not straightforward; however, one can obtain FRET signatures for specific transcription complexes (that can be preferentially formed upon addition of DNA and nucleotide subsets) and then monitor the transitions between the calibrated FRET states.

To check whether static quenching is a contributing mechanism for the observed quenching, we recorded the absorbance spectra of free Cy3B and DNA (Figure S7 of the Supporting Information). The results show that the absorption maximum of Cy3B (≈560 nm) is blue-shifted to ≈548 nm when ATTO647N is present (Figure S7 of the Supporting Information). This blue shift is an indication of the presence of static quenching based on the formation of H-dimers, as discussed previously (*32*). The observed quenching can, however, also be in part due to (i) contact-induced quenching of both fluorophores with a dynamic origin (*32*) or (ii) DNA-mediated photoinduced electron transfer (*33*−*35*).

We also performed experiments at the single-molecule level using ALEX spectroscopy. Upon addition of either 50% (v/v) ethanol (Figure 3b) or 1.5 mM SDS (Figure 3c), contact-induced quenching seen in dsDNA (Figure 3a) is eliminated and distributions with very high FRET values emerge (maximal $E^* > 0.9$).

We observe that dequenching appears to have distinct threshold concentrations of ≈30% (v/v) ethanol and ≈0.75 mM SDS (data not shown). To rule out specific interactions between SDS and the two fluorophores, similar experiments were performed using the same FRET pair with an 18 bp separation; no FRET change was observed upon addition of SDS (Figure S3 of the Supporting Information). Our findings provide strong support for the presence of contact-induced quenching in dsDNA and the dequenching caused by either surfactants or partial opening of DNA, e.g., due to RP_o formation. The observed dequenching is possibly due to the attenuation of hydrophobic interactions between the two fluorophores and the formation of a solvation shell around the fluorophores caused by favorable interactions between ethanol or SDS and hydrophobic parts of the fluorophore molecules (*32*). While revealing the exact underlying mechanism causing our observations is worthy of a study in its own right, we chose to focus our efforts in applying the assay to provide insight into biological systems. A more detailed description of the underlying dye photophysics is found in refs (*32*−*35*) and could be the principal subject of a future publication.

Monitoring the Kinetics of Promoter Opening Using quFRET. Kinetic analysis of transcription on different promoters and promoter-proximal regions can establish rate-limiting steps that modulate transcription either by endogenous factors or by small molecules that can serve as antibacterial agents. In initial transcription, this step is often the isomerization from a closed RNAP-DNA complex to RP_o (*12*−*15*). To follow the kinetics of RP_o formation, we monitored the time dependence of the ensemble FRET signal increase due to fluorophore dequenching in $lac^{Cy3B,-5/ATTO647N,-3}$ (Figure 4).

Upon mixing $lac^{Cy3B,-5/ATTO647N,-3}$ (20 nM) with the RNAP holoenzyme (100 nM) at 37 °C, we observe a biexponential increase in fluorescence intensity due to RP_o formation. The measured rate constants of four individual experiments show the following mean values: $k_1 = (63 \pm 56) \times 10^{-3}\ s^{-1}$ (amplitude of 45%), and $k_2 = (4.9 \pm 2.8) \times 10^{-3}\ s^{-1}$ (amplitude of 55%). The rates are in good agreement with published values for a related promoter (*lac*UV5) determined using a gel shift assay where biexponential kinetics were also observed ($k_1 = 118 \times 10^{-3}\ s^{-1}$ with an amplitude of 60%, interpreted as formation of closed complexes, and $k_2 = 12 \times 10^{-3}\ s^{-1}$ with an amplitude of 40%, interpreted as isomerization) (*12*). The 2-fold difference between the studies may reflect measurement errors (partly due to manual mixing) and the differences between the *lac* sequences used in the two studies (*36*).

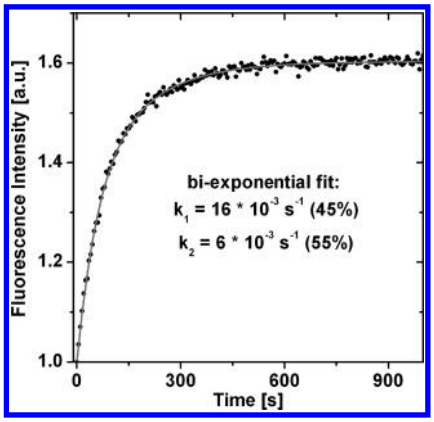

FIGURE 4: quFRET monitors the kinetics of RP_o formation. Relative increases in the magnitude of the fluorescence signal at 660 nm upon excitation at 533 nm (circles). At time zero, the RNAP holoenzyme (100 nM) was added and rapidly mixed with dsDNA (20 nM) at 37 °C. A biexponential fit (gray line) yielded two rate constants for RP_o formation with the fit parameters shown; repeated experiments led to values of $(63 \pm 56) \times 10^{-3}\ s^{-1}$ (amplitude of 45%) and $(4.9 \pm 2.8) \times 10^{-3}\ s^{-1}$ (amplitude of 55%).

Our results establish the ability of quFRET to monitor the kinetics of promoter opening in a simple yet quantitative fashion. The full compatibility of this assay with single-molecule fluorescence detection should allow monitoring of the kinetics of promoter opening at the level of diffusing single molecules [with a temporal resolution of minutes (*29*)] or at the level of immobilized single molecules with millisecond time resolution (*37*).

Monitoring Abortive Transcription and Promoter Escape Using quFRET. Mechanistic steps occurring after RP_o formation, such as abortive initiation (i.e., the reiterative synthesis and release of RNA transcripts two to nine nucleotides in length by initial transcribing complexes, RP_{itc}), also change the size and shape of the transcription bubble. Prior work in our laboratory (*23*) and by others (*17*) showed that abortive initiation by bacterial RNAP proceeds by a DNA scrunching mechanism, involving formation and dissolution of transient bulged or looped DNA structures within the transcription bubble. Neither of the methods, however, observed DNA scrunching directly; also unclear is which parts of the bubble move (or become scrunched) during abortive initiation. We thus tested whether quFRET can provide a means of addressing these questions.

To probe DNA conformational changes using quFRET, we used the DNA fragment $lac^{Cy3B,-5/ATTO647N,-3}$, which carries both fluorophores within the transcription bubble of RP_o. We prepared initial transcribing complexes capable of synthesizing abortive RNA of different maximum lengths by using nucleotide subsets dictated by the initial transcribed sequence of our *lac* fragment (Materials and Methods) and observing their smFRET signatures (Figure 5).

Upon addition of 500 μM initiating dinucleotide ApA to RP_o, we formed complex $RP_{itc,2}$ (equivalent to a transcription complex in which RNAP has synthesized the first dinucleotide, pppApA); FRET analysis of the donor−acceptor species showed a distinct FRET peak with a mean E^* of ≈0.68 (a value essentially identical to that of RP_o; compare to Figure 1b) and a standard deviation of

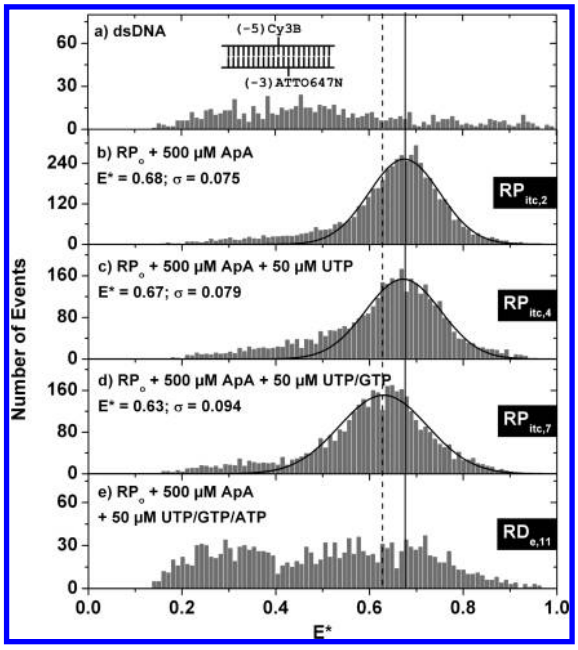

FIGURE 5: Monitoring initial transcription and promoter escape using quFRET. ALEX-based E^* histograms of single diffusing molecules of transcription complexes formed using lac$^{Cy3B,-5/ATTO647N,-3}$ DNA at 37 °C and at a DNA concentration of ≈50−100 pM. The nucleotide subsets added to the RP_o and the transcription complexes thus formed are indicated in the different panels. Measurement times for the different panels were ≈90 min for panels a and b, ≈120 min for panels c and d, and ≈30 min for panel e.

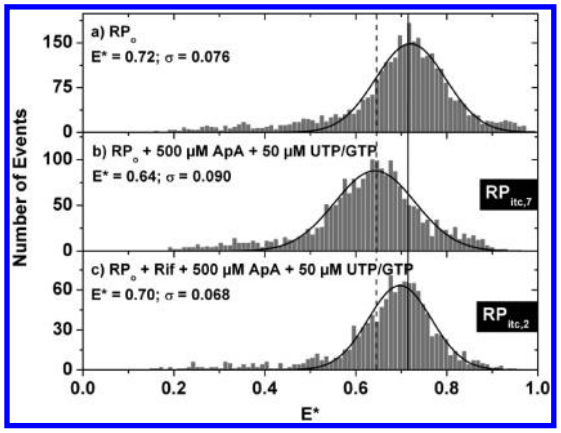

FIGURE 6: quFRET can detect the activity of the antibiotic rifampicin. ALEX-based E^* histograms of single diffusing molecules of transcription complexes formed using lac$^{Cy3B,-5/ATTO647N,-3}$ DNA at 37 °C and at a DNA concentration of ≈50−100 pM. The presence of different nucleotides in the buffer is indicated in the different panels. In the bottom panel, the antibiotic rifampicin (Rif) was added at a concentration of 250 nM to prevent the transcription complex from producing abortive transcripts more than two nucleotides in length. The measurement time was ≈30−40 min for each panel.

0.075 (Figure 5b). Addition of UTP, the nucleotide complementary to bases 3 and 4 in our *lac* template sequence (Figure 1a), leads to the formation of initial transcribing complex $RP_{itc,4}$ (capable of synthesizing RNA of up to four nucleotides in length); this complex is characterized by a small shift in FRET and a slight increase in width (Figure 5c). More significantly, upon addition of 50 μM UTP and 50 μM GTP to RP_o for formation of the initial transcribing complex $RP_{itc,7}$ (capable of synthesizing RNA up to seven nucleotides in length), we see a significant E^* decrease to ≈0.63, as well as broadening of the distribution [standard deviation of 0.094 (Figure 5d)]. These results clearly establish our ability to distinguish between the FRET signatures of RP_o, $RP_{itc,2}$, and $RP_{itc,4}$ and the signature of $RP_{itc,7}$. Similar results [i.e., decrease in apparent FRET and distribution broadening upon movement from $RP_{itc,2}$ to $RP_{itc,7}$ (see Figure S6 of the Supporting Information)] were obtained for a different labeling position on the *lac* fragment (lac$^{Cy3B,-3/ATTO647N,-3}$ DNA, in which the donor is incorporated at position −3 on the nontemplate strand).

Interestingly, we observe FRET decreases between RP_o, $RP_{itc,2}$, and $RP_{itc,4}$ and the signature of $RP_{itc,7}$ for both DNAs examined (lac$^{Cy3B,-5/ATTO647N,-3}$ and lac$^{Cy3B,-3/ATTO647N,-3}$); similar results have also been obtained in FRET measurements between positions −15 and −3 on the nontemplate strand (L. C. Hwang and A. N. Kapanidis, unpublished observations). These results from quFRET in combination with additional systematic smFRET experiments within several RP_{itc} complexes of the bacterial RNAP should allow identification of the position and dynamics of scrunched DNA in the initial transcription for multisubunit RNAP. In a future publication, we intend to compare the predictions and validity of different models, e.g., the "steric exclusion model" (*23*, *38*), which describes scrunching in the RNAP initiation complexes, where the scrunched DNA is accommodated within or close to the active site pocket of RNAP, or other existing models (*39*, *40*).

We also considered whether our FRET pair can sense the downstream movement of the transcription bubble upon promoter escape and formation of RNAP−DNA elongation complexes (RD_e) (*2*, *3*). To form the first stable elongation complex ($RD_{e,11}$, a stable elongation complex in which RNAP has synthesized an 11-mer RNA transcript still bound within the complex), we added UTP, GTP, and ATP to RP_o. In this case, although the DNA between the two fluorophores is expected to reclose, it was unclear whether the quenched state would be reformed, since the local presence of protein residues may affect quenching in a manner similar to that of ethanol or SDS. Our results for $RD_{e,11}$ show a broad E^* distribution, but with many more donor−acceptor molecules than in free DNA (Figure 5e, with a measurement duration 3-fold shorter than that for Figure 5a). Our result most likely represents a mixture of species: elongation complexes that escape to elongation and assume a fully or partially quenched state, transcription complexes unable to escape to elongation [with this species ranging from ≈15 to 40% (*23*, *41*, *42*)], and free DNA molecules due to heparin challenge. Further experiments with immobilized molecules will help distinguish between such subpopulations.

To confirm that the observed FRET changes in initial transcription and elongation are due to transcription reactions, we performed control experiments using rifampicin, an antibiotic that prevents synthesis of RNA transcripts longer than two or three nucleotides (Figure 6), even in the presence of all four nucleotides (*43*).

Indeed, preincubation of RNAP with rifampicin before RP_o and $RP_{itc,7}$ formation (Figure 6c) abolishes the 8% decrease in E^* seen upon the addition of UTP and GTP to RP_o (to form $RP_{itc,7}$) in the absence of rifampicin (Figure 6a,b). These results establish that the FRET changes shown in Figures 5 and 6 are due to RNA synthesis and conformational changes in DNA. These experiments also show that quFRET can be used to study the mode of action of antibiotics that block initial transcription and promoter escape and to screen novel antimicrobial compounds that target transcription.

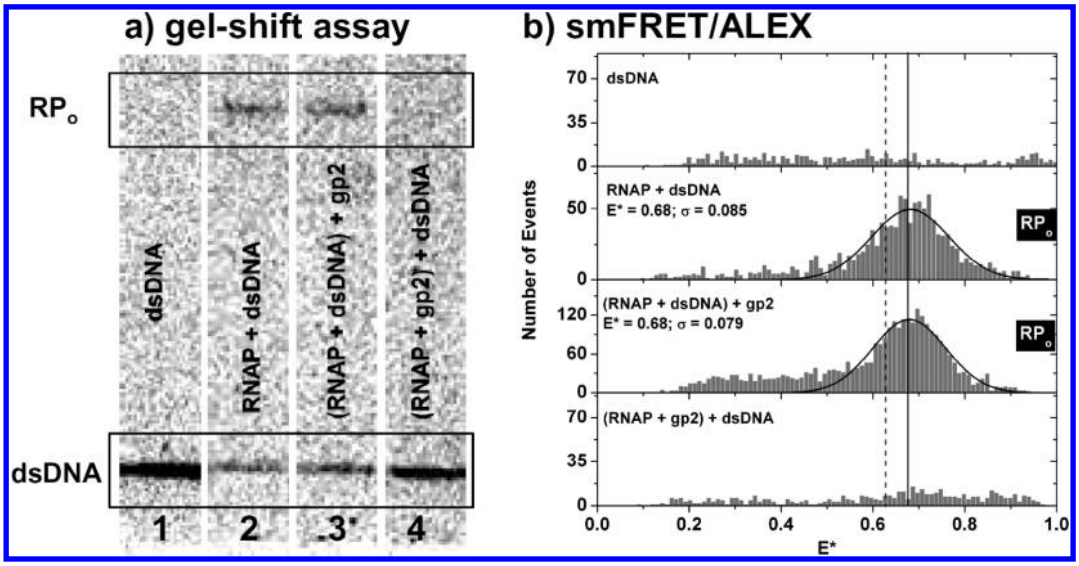

FIGURE 7: gp2 inhibits transcription by preventing DNA opening. (a) Results of gp2 inhibition of RP_o formation at $lac^{Cy3B,-5/ATTO647N,-3}$ using gel electrophoresis; the images shows acceptor emission upon acceptor excitation (a signal that is not affected by FRET but is affected by contact-induced quenching). Different lanes correspond to different sample mixtures or orders of addition: (1) dsDNA only, (2) dsDNA and RNAP, with heparin Sepharose challenge, (3) dsDNA, RNAP, and gp2, with heparin Sepharose challenge, and (4) RNAP, gp2, and dsDNA, with heparin Sepharose challenge. (b) ALEX-based E^* histograms of single diffusing molecules of transcription complexes formed using $lac^{Cy3B,-5/ATTO647N,-3}$ DNA at 37 °C and a DNA concentration of ≈50−100 pM. The panels show apparent FRET of samples found in gel lanes 1−4 (panel a) as indicated in the figure. The measurement time was ≈30−40 min for each panel.

Using quFRET To Study the Mechanism of a Specific Inhibitor of Promoter Opening. To demonstrate the ability of quFRET to study protein−protein interactions that modulate transcription, we studied the mechanism by which gp2, a small T7 phage-encoded protein and potent inhibitor of *E. coli* RNAP, blocks transcription (*44*). Recent experiments have suggested that gp2-based inhibition involves prevention of RNAP−promoter DNA interactions required for strand separation and formation of the transcription bubble (*44*).

To test the proposed mechanism of gp2 action, we used quFRET on $lac^{Cy3B,-5/ATTO647N,-3}$. To establish whether the fluorophores perturb the inhibitory activity of gp2 on formation of RNAP−promoter DNA complexes, we performed a gel mobility shift assay (Figure 7a, native gel electrophoresis).

As expected, gp2 cannot disrupt preformed RNAP−DNA complexes (Figure 7a, lane 3).When preincubated with RNAP alone, however, before addition of promoter DNA, gp2 prevents RP_o formation (Figure 7a, lane 4). These results are in agreement with published results (*44*) and indicate that the fluorophores do not interfere with gp2 activity.

To test whether quFRET can identify the gp2 mode of action, we examined the effect of gp2 addition using quFRET (Figure 7b). Free dsDNA ($lac^{Cy3B,-5/ATTO647N,-3}$) shows the broad featureless FRET distribution (Figure 7b, top panel) seen in Figures 1a and 5. As expected, RP_o formation is evident as a distinct FRET peak at 0.68 (Figure 7b, second panel); an identical FRET signature is obtained when we first form RP_o via incubation of RNAP with dsDNA and then addition of gp2. In contrast, no RP_o formation is seen when gp2 and RNAP are preincubated before the addition of promoter DNA (Figure 7b, bottom panel; conditions comparable to those in lane 4 of Figure 7a). This is evident by the very small number of molecules with E^* values of ≈0.7, i.e., the region populated by the RP_o for $lac^{Cy3B,-5/ATTO647N,-3}$ (Figures 1 and 2). Our results provide strong support for recent work showing that gp2 prevents bacterial transcription by blocking steps along the formation of RP_o (*44*). Our results additionally demonstrate that quFRET can be used as a sensitive and versatile tool for screening mutant versions of gp2 or a library of gp2 mimetics for their ability to inhibit the RNAP.

Comparison of quFRET and Conventional smFRET. What are the studies that will benefit from the unique features of quFRET versu conventional smFRET? First, one should consider that in cases of donor−acceptor proximity (either due to constraints in experimental design or due to limited information about molecular conformations), quenching is a very real possibility that has to be characterized (*32*−*35*), understood, and, if possible, turned into a tool. If such quenching remains undetected, it is likely that a significant faction of donor−acceptor molecules may be absent from the FRET histograms; FRET will hence not be a reliable ruler, and FRET monitoring cannot be used for kinetic studies without modification of standard analysis methods.

Second, the proximity afforded by quFRET fluorophore pairs results in a very large signal during processes such as DNA opening; this large signal of quFRET is accompanied by the ability to monitor conformational changes within DNA (which relies on conventional smFRET) and on top of changes in the local environment of the fluorophores [e.g., due to PIFE (*17*)], effects that can be monitored using ALEX-based direct monitoring of both fluorophores.

Finally, the suppression of the fluorescence signal in the absence of DNA opening allows studies of rare events that can be observed in the presence of high concentrations of a DNA probe. The quFRET assay also provides a no-background scenario that can be used to look at rare promoter opening events in constrained situations, such as in bacterial cells loaded with quFRET sensors (a measurement that is very difficult using standard smFRET techniques).

CONCLUSIONS

We introduced a FRET-based assay capable of monitoring the local state of DNA (single- vs double-stranded) both at the ensemble and single-molecule levels. The assay requires the

attachment of two fluorophores in proximity, one on each strand of the dsDNA under study. While quFRET is unlikely to be compatible with every FRET pair, we have shown that the pair of Cy3B and ATTO647N (which are excellent fluorophores for single-molecule experiments) is a robust pair for this new assay. We anticipate that future work will identify additional fluorophore pairs for quFRET; in particular, it would be desirable to identify quFRET-compatible fluorophores in the blue spectral range, because they are smaller moieties and, as such, less likely to interfere with biological function.

We presented different applications and a photophysical rationale for quFRET's working principle. We showed that quFRET can monitor initial transcription, e.g., RP_o formation, and bubble expansion and compaction during initial transcription. The quFRET assay allowed us to monitor the kinetics of binding of bacterial RNAP to *lac* promoter DNA and to study the mode of action of small proteins and antibiotics that block different steps in transcription initiation and initial transcription. The latter results established that quFRET will find numerous applications not only in mechanistic studies but also in the development of new antibacterial therapies. This work also lays the foundation for using quFRET for the real-time detection of abortive initiation and promoter escape using surface-immobilized transcription complexes.

SUPPORTING INFORMATION AVAILABLE

DNA oligonucleotide sequences and additional experimental results. This material is available free of charge via the Internet at http://pubs.acs.org.

REFERENCES

1. Orphanides, G., and Reinberg, D. (2002) A unified theory of gene expression. *Cell 108*, 439–451.
2. Murakami, K. S., and Darst, S. A. (2003) Bacterial RNA polymerases: The wholo story. *Curr. Opin. Struct. Biol. 13*, 31–39.
3. Young, B. A., Gruber, T. M., and Gross, C. A. (2002) Views of transcription initiation. *Cell 109*, 417–420.
4. Buc, H., and McClure, W. R. (1985) Kinetics of open complex formation between *Escherichia coli* RNA polymerase and the lac UV5 promoter. Evidence for a sequential mechanism involving three steps. *Biochemistry 24*, 2712–2723.
5. Revyakin, A., Ebright, R. H., and Strick, T. R. (2004) Promoter unwinding and promoter clearance by RNA polymerase: Detection by single-molecule DNA nanomanipulation. *Proc. Natl. Acad. Sci. U.S.A. 101*, 4776–4780.
6. Borowiec, J. A., Zhang, L., Sasse-Dwight, S., and Gralla, J. D. (1987) DNA supercoiling promotes formation of a bent repression loop in lac DNA. *J. Mol. Biol. 196*, 101–111.
7. Kirkegaard, K., Buc, H., Spassky, A., and Wang, J. C. (1983) Mapping of single-stranded regions in duplex DNA at the sequence level: Single-strand-specific cytosine methylation in RNA polymerase-promoter complexes. *Proc. Natl. Acad. Sci. U.S.A. 80*, 2544–2548.
8. Sclavi, B., Woodson, S., Sullivan, M., Chance, M. R., and Brenowitz, M. (1997) Time-resolved synchrotron X-ray "footprinting", a new approach to the study of nucleic acid structure and function: Application to protein-DNA interactions and RNA folding. *J. Mol. Biol. 266*, 144–159.
9. Sclavi, B., Zaychikov, E., Rogozina, A., Walther, F., Buckle, M., and Heumann, H. (2005) Real-time characterization of intermediates in the pathway to open complex formation by *Escherichia coli* RNA polymerase at the T7A1 promoter. *Proc. Natl. Acad. Sci. U.S.A. 102*, 4706–4711.
10. Sylvester, J. E., and Cashel, M. (1980) Stable RNA-DNA-RNA Polymerase Complexes Can Accompany Formation of a Single Phosphodiester Bond. *Biochemistry 19*, 1069–1074.
11. Callaci, S., and Heyduk, T. (1998) Conformation and DNA binding properties of a single-stranded DNA binding region of σ70 subunit from *Escherichia coli* RNA polymerase are modulated by an interaction with the core enzyme. *Biochemistry 37*, 3312–3320.
12. Matlock, D. L., and Heyduk, T. (1999) A real-time fluorescence method to monitor the melting of duplex DNA during transcription initiation by RNA polymerase. *Anal. Biochem. 270*, 140–147.
13. Jia, Y., Kumar, A., and Patel, S. S. (1996) Equilibrium and stopped-flow kinetic studies of interaction between T7 RNA polymerase and its promoters measured by protein and 2-aminopurine fluorescence changes. *J. Biol. Chem. 271*, 30451–30458.
14. Sastry, S. S., and Ross, B. M. (1996) A direct real-time spectroscopic investigation of the mechanism of open complex formation by T7 RNA polymerase. *Biochemistry 35*, 15715–15725.
15. Sullivan, J. J., Bjornson, K. P., Sowers, L. C., and deHaseth, P. L. (1997) Spectroscopic determination of open complex formation at promoters for *Escherichia coli* RNA polymerase. *Biochemistry 36*, 8005–8012.
16. Kapanidis, A. N., and Strick, T. (2009) Biology, one molecule at a time. *Trends Biochem. Sci. 34*, 234–243.
17. Myong, S., Bruno, M. M., Pyle, A. M., and Ha, T. (2007) Spring-loaded mechanism of DNA unwinding by hepatitis C virus NS3 helicase. *Science 317*, 513–516.
18. Revyakin, A., Liu, C., Ebright, R. H., and Strick, T. R. (2006) Abortive initiation and productive initiation by RNA polymerase involve DNA scrunching. *Science 314*, 1139–1143.
19. Hohlbein, J., Gryte, K., Heilemann, M., and Kapanidis, A. N. (2010) Surfing on a new wave of single-molecule fluorescence methods. *Phys. Biol. 7*, 031001.
20. Merrick, M. J. (1993) In a class of its own: The RNA polymerase sigma factor sigma 54 (sigma N). *Mol. Microbiol. 10*, 903–909.
21. Tjian, R. (1996) The biochemistry of transcription in eukaryotes: A paradigm for multisubunit regulatory complexes. *Philos. Trans. R. Soc. London, Ser. B 351*, 491–499.
22. Holden, S. J., Uphoff, S., Hohlbein, J., Yadin, D., Le Reste, L., Britton, O. J., and Kapanidis, A. N. (2010) Defining the limits of single-molecule FRET resolution in TIRF microscopy. *Biophysical J. 99*, 9 (in press).
23. Kapanidis, A. N., Margeat, E., Ho, S. O., Kortkhonjia, E., Weiss, S., and Ebright, R. H. (2006) Initial transcription by RNA polymerase proceeds through a DNA-scrunching mechanism. *Science 314*, 1144–1147.
24. Kapanidis, A. N., Margeat, E., Laurence, T. A., Doose, S., Ho, S. O., Mukhopadhyay, J., Kortkhonjia, E., Mekler, V., Ebright, R. H., and Weiss, S. (2005) Retention of Transcription Initiation Factor σ^{70} in Transcription Elongation: Single-Molecule Analysis. *Mol. Cell 20*, 347–356.
25. Vogelsang, J., Cordes, T., and Tinnefeld, P. (2009) Single-molecule photophysics of oxazines on DNA and its application in a FRET switch. *Photochem. Photobiol. Sci. 8*, 486–496.
26. Santoso, Y., Joyce, C. M., Potapova, O., Le Reste, L., Hohlbein, J., Torella, J. P., Grindley, N. D. F., and Kapanidis, A. N. (2010) Conformational transitions in DNA polymerase I revealed by single-molecule FRET. *Proc. Natl. Acad. Sci. U.S.A. 107*, 715–720.
27. Santoso, Y., and Kapanidis, A. N. (2009) Probing Biomolecular Structures and Dynamics of Single Molecules Using In-gel Alternating-Laser Excitation. *Anal. Chem. 81*, 9561–9570.
28. Kapanidis, A. N., Laurence, T. A., Lee, N. K., Margeat, E., Kong, X., and Weiss, S. (2005) Alternating-laser excitation of single molecules. *Acc. Chem. Res. 38*, 523–533.
29. Kapanidis, A. N., Lee, N. K., Laurence, T. A., Doose, S., Margeat, E., and Weiss, S. (2004) Fluorescence-aided molecule sorting: Analysis of structure and interactions by alternating-laser excitation of single molecules. *Proc. Natl. Acad. Sci. U.S.A. 101*, 8936–8941.
30. Eggeling, C., Berger, S., Brand, L., Fries, J. R., Schaffer, J., Volkmer, A., and Seidel, C. A. (2001) Data registration and selective single-molecule analysis using multi-parameter fluorescence detection. *J. Biotechnol. 86*, 163–180.
31. Kong, X. X., Nir, E., Hamadani, K., and Weiss, S. (2007) Photobleaching pathways in single-molecule FRET experiments. *J. Am. Chem. Soc. 129*, 4643–4654.
32. Brune, R., Doose, S., and Sauer, M. (2007) Analyzing the influence of contact-mediated quenching processes on Förster resonance energy transfer. In Progress in Biomedical Optics and Imaging, pp 6633−6657, Optical Society of America, Baltimore.
33. Di Fiori, N., and Meller, A. (2010) The effect of dye-dye interactions on the spatial resolution of single-molecule FRET measurements in nucleic acids. *Biophys. J. 98*, 2265–2272.
34. Kumbhakar, M., Kiel, A., Pal, H., and Herten, D. P. (2009) Single-molecule fluorescence studies reveal long-range electron-transfer dynamics through double-stranded DNA. *ChemPhysChem 10*, 629–633.
35. Doose, S., Neuweiler, H., and Sauer, M. (2009) Fluorescence quenching by photoinduced electron transfer: A reporter for conformational dynamics of macromolecules. *ChemPhysChem 10*, 1389–1398.

36. Gralla, J. D., Carpousis, A. J., and Stefano, J. E. (1980) Productive and abortive initiation of transcription in vitro at the lac UV5 promoter. *Biochemistry 19*, 5864–5869.
37. Margeat, E., Kapanidis, A. N., Tinnefeld, P., Wang, Y., Mukhopadhyay, J., Ebright, R. H., and Weiss, S. (2006) Direct observation of abortive initiation and promoter escape within single immobilized transcription complexes. *Biophys. J. 90*, 1419–1431.
38. Roberts, J. W. (2006) Biochemistry. RNA polymerase, a scrunching machine. *Science 314*, 1097–1098.
39. Cheetham, G. M., and Steitz, T. A. (1999) Structure of a transcribing T7 RNA polymerase initiation complex. *Science 286*, 2305–2309.
40. Tang, G. Q., Roy, R., Ha, T., and Patel, S. S. (2008) Transcription initiation in a single-subunit RNA polymerase proceeds through DNA scrunching and rotation of the N-terminal subdornains. *Mol. Cell 30*, 567–577.
41. Mukhopadhyay, J., Kapanidis, A. N., Mekler, V., Kortkhonjia, E., Ebright, Y. W., and Ebright, R. H. (2001) Translocation of σ^{70} with RNA polymerase during transcription: Fluorescence resonance energy transfer assay for movement relative to DNA. *Cell 106*, 453–463.
42. Kubori, T., and Shimamoto, N. (1996) A branched pathway in the early stage of transcription by *Escherichia coli* RNA polymerase. *J. Mol. Biol. 256*, 449–457.
43. Campbell, E. A., Korzheva, N., Mustaev, A., Murakami, K., Nair, S., Goldfarb, A., and Darst, S. A. (2001) Structural mechanism for rifampicin inhibition of bacterial RNA polymerase. *Cell 104*, 901–912.
44. Camara, B., Liu, M., Reynolds, J., Shadrin, A., Liu, B., Kwok, K., Simpson, P., Weinzierl, R., Severinov, K., Cota, E., Matthews, S., and Wigneshweraraj, S. R. (2010) T7 phage protein Gp2 inhibits the *Escherichia coli* RNA polymerase by antagonizing stable DNA strand separation near the transcription start site. *Proc. Natl. Acad. Sci. U.S.A. 107*, 2247–2252.